Correlating material-specific layers and magnetic distributions within onion-like $Fe_3O_4/MnO/\gamma$-Mn_2O_3 core/shell nanoparticles

K. L. Krycka,[1,a)] J. A. Borchers,[1] M. Laver,[2] G. Salazar-Alvarez,[3] A. López-Ortega,[4] M. Estrader,[3] S. Suriñach,[5] M. D. Baró,[5] J. Sort,[5,6] and J. Nogués[4,6]
[1]*Center for Neutron Research, NIST, Gaithersburg, Maryland 20899, USA*
[2]*Paul Scherrer Institute, 5232 Villigen, Switzerland*
[3]*Department of Materials and Environmental Chemistry, Stockholm University, S-10691 Stockholm, Sweden*
[4]*CIN2(ICN-CSIC) and Universitat Autònoma de Barcelona, Catalan Institute of Nanotechnology (ICN), Campus de la UAB, E-08193 Bellaterra (Barcelona), Spain*
[5]*Departament de Física, Universitat Autònoma de Barcelona, E-08193 Bellaterra, Spain*
[6]*Institució Catalana de Recerca i Estudis Avançats (ICREA), Barcelona, Spain*

(Presented 18 January 2013; received 5 November 2012; accepted 4 February 2013; published online 19 April 2013)

The magnetic responses of two nanoparticle systems comprised of Fe_3O_4/γ-Mn_2O_3 (soft ferrimagnetic, FM/hard FM) and $Fe_3O_4/MnO/\gamma$-Mn_2O_3 (soft FM/antiferromagnetic, AFM/hard FM) are compared, where the MnO serves to physically decouple the FM layers. Variation in the temperature and applied field allows for Small Angle Neutron Scattering (SANS) measurements of the magnetic moments both parallel and perpendicular to an applied field. Data for the bilayer particle indicate that the graded ferrimagnetic layers are coupled and respond to the field as a single unit. For the trilayer nanoparticles, magnetometry suggests a Curie temperature (T_C) $\approx$ 40 K for the outer γ-Mn_2O_3 component, yet SANS reveals an increase in the magnetization associated with outer layer that is perpendicular to the applied field above T_C during magnetic reversal. This result suggests that the γ-Mn_2O_3 magnetically reorients relative to the applied field as the temperature is increased above 40 K. © *2013 AIP Publishing LLC* [http://dx.doi.org/10.1063/1.4801423]

Magnetic nanoparticles have drawn a great deal of interest for applications in biology and material science.[1–3] Since the report on the use of exchange bias to overcome the superparamagnetic limit in magnetic storage,[4] interest in core-shell exchange-coupled nanoparticles has surged.[5–7] To date, most of the studied systems consist of ferromagnetic or ferrimagnetic (FM) cores with antiferromagnetic (AFM) passivation shells.[5,8–10] Advances in chemical synthesis allowing the controlled growth of more complex nanoparticles have triggered interest in core/shell and onion-like magnetic nanoparticles.[11–15] Studies on hard/soft core/shell nanoparticles are revealing interesting magnetic properties such as reversible tuning of the blocking temperature,[14] enhanced coercivity,[13] improved microwave absorption,[16] or optimized hyperthermia.[17] Despite their potential to tailor the magnetic properties, the studies on onion-like, magnetic nanoparticles are rather scarce[15] due to, in part, the difficulty in synthesizing these structures.

Here, we compare and contrast the magnetic response of two systems nominally comprised of 3 nm diameter Fe_3O_4 core/2.5 nm thick γ-Mn_2O_3 shell nanoparticles (S_0) and 6 nm diameter Fe_3O_4 core/30 nm MnO thick shell/5 nm thick γ-Mn_2O_3 shell nanoparticles (S_{30}). Small Angle Neutron Scattering (SANS) provides detailed information regarding their magnetic morphologies. Variation in temperature and field allows analysis of FM and AFM responses.

The nanoparticles have been synthesized by seeded growth, where monodispersed Fe_3O_4 nanoparticles were used as seeds for the subsequent growth of manganese oxide.[12,15] Different amounts of MnO were layered on the Fe_3O_4 seeds by thermal decomposition of manganese (II) acetylacetonate. The MnO is then passivated in air leading to a thin layer of γ-Mn_2O_3, nominally Fe_3O_4/γ-Mn_2O_3 and $Fe_3O_4/MnO/\gamma$-Mn_2O_3 for thin and thick manganese oxide overlayers, respectively. For S_0 anomalous x-ray diffraction reveals that the resulting nanoparticles are 8.2 nm ± 0.2 nm in diameter and consist in the ensemble average of a small Fe_3O_4 core surrounded by a graded $(Mn_XFe_{1-X})_3O_4$ shell ranging from X = 0.40 to 0.46.[18] High resolution transmission electron microscopy (HR-TEM) with electron energy loss spectroscopy[19] confirms the core/shell and onion-like morphology and indicates that the outermost edge of the nanoparticles transition to γ-Mn_2O_3. Thus, S_0 is entirely ferrimagnetic, composed of a soft core (Fe_3O_4) and a hard shell (γ-Mn_2O_3) or, to a certain extent, a graded anisotropy similar to thin film systems.[20] On the other hand, sample S_{30} is composed of a hard-FM/AFM/soft-FM. Thus, we have two comparative nanoparticle systems with and without an intermediate AFM spacer layer of MnO between FM core and FM outer shell. X-ray diffraction shows clear signature of Fe_3O_4 and MnO peaks in S_{30}, but no readily identifiable γ-Mn_2O_3 (or Mn_3O_4) peaks, leading us to conclude that the γ-Mn_2O_3 shell remains thin. HR-TEM indicates that the S_{30} nanoparticles are 80 nm ± 10 nm in diameter, accompanied by some uncoated Fe_3O_4 seeds (≈6 nm in diameter). SANS probes magnetism, both in magnitude and spatial distribution as a function of applied magnetic field or temperature. Polarization Analyzed SANS (PASANS)[21] additionally offers the ability to measure the net magnetic direction of distinctive layers, although it limits the applied field magnitude. All neutron measurements were performed at NIST Center for Neutron Research (NCNR), beamlines NG3 and NG7.

a)Author to whom correspondence should be addressed. Electronic mail: kathryn.krycka@nist.gov.

PASANS was performed with an electromagnet capable of reaching 1.25 T. Detection of the neutron spin prior to and after sample scattering was achieved using a combination of a FeSi supermirror, an electromagnetic spin flipper, and a ^{3}He spin analyzing cell. As shown in Fig. 1, four conditions of S_0 were examined: 0.005 T and 1.2 T at 5 K and 100 K. The scattering involving neutrons whose spins are not reversed (non spin-flip) allows for the extraction of the magnetic moments parallel to the applied field,[21,22] $|M_{\parallel}|^2$. Fig. 1(a) reveals that $|M_{\parallel}|^2$ closely follows the scattering from the nanoparticle structure (open circles) with a nearest-neighbor peak observed at 0.085 Å^{-1}. The presence of a sharp peak indicates that these particles are tightly packed and have a well-defined structural order. $|M_{\parallel}|^2$ decreases with increased temperature or decreased field. (Error bars in all figures denote one standard deviation.)

Scattering from neutrons whose spins are reversed (spin-flip) allows for the extraction of the scattering from magnetic moments perpendicular to the applied field,[21,22] $|M_{\perp}|^2$, Fig. 1(b). $|M_{\perp}|^2$ is almost absent in a field of 1.25 T (i.e., near saturation) regardless of temperature. At 0.005 T, $|M_{\perp}|^2$ increases slightly at 5 K. At 100 K, the scattering is no longer dominated by multi-particle correlations (i.e., the diffraction peak is absent), but rather reflects the magnetic morphology of individual particles. The 100 K, 0.005 T data minus the 5 K, 1.2 T data (serving as the incoherent scattering background) can be modeled with a uniform sphere[23] of 8.4 nm in diameter, Fig. 1(b) inset. Note that $|M_{\perp}|^2$ is inversely proportional to $|M_{\parallel}|^2$ as a function of temperature. This suggests that the magnetic moments from both the Fe_3O_4 and γ-Mn_2O_3 layers rotate uniformly upon relaxation in a remnant field. This is consistent with recent studies on similar core/shell samples, where it was shown that given the small size of the soft counterpart, the core and the shell are strongly exchange coupled and reverse coherently[12] in agreement with thin film systems.[24]

S_{30} requires a larger field to achieve saturation, and thus, was measured with an unpolarized neutron beam in a superconducting magnet field of up to ±7 T. The sample was field cooled at −5 T to 5 K, increased to 7 T, decreased to −7 T, and then measured in order at −1.5 T, 0.2 T, 1.5 T, and 7 T. After that the sample was warmed to 150 K, then recooled to 50 K at −7 T before being measured in order at 0.2 T and 7 T. The first structural peak at 0.007 Å^{-1} (Fig. 2(a)) is correlated with the trilayer particles, while the higher-Q scattering around ≈0.1 Å^{-1} would be consistent with scattering coming from smaller features, such as the Fe_3O_4 cores or seeds. As the field and temperature are varied, the scattering is dominated by structural scattering and does not noticeably vary. However, subtraction of one field and/or temperature state from another can effectively remove the structural scattering while highlighting changes in magnetic morphology. No

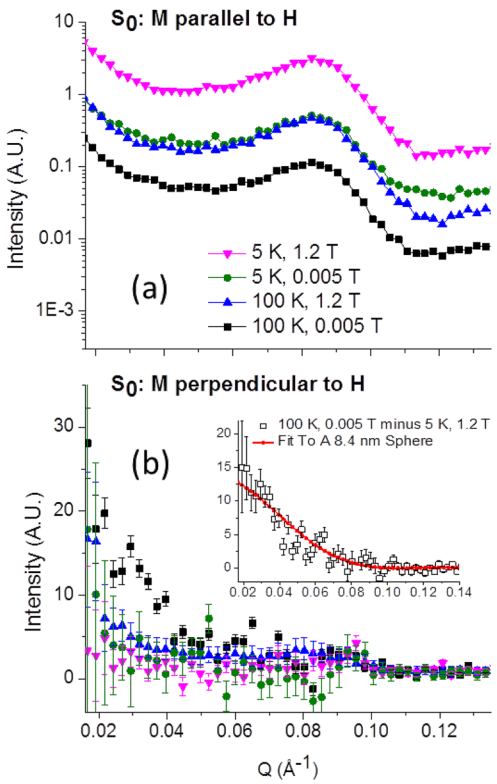

FIG. 1. SANS profiles for S_0 at 0.005 T and 1.25 T, 5 K and 100 K with (a) $|M_{\parallel}|^2$, (b) $|M_{\perp}|^2$. Inset shows that the magnetic difference between 100 K, 0.005 T and 5 K, 1.2 T can be modeled with an 8.4 nm diameter sphere.

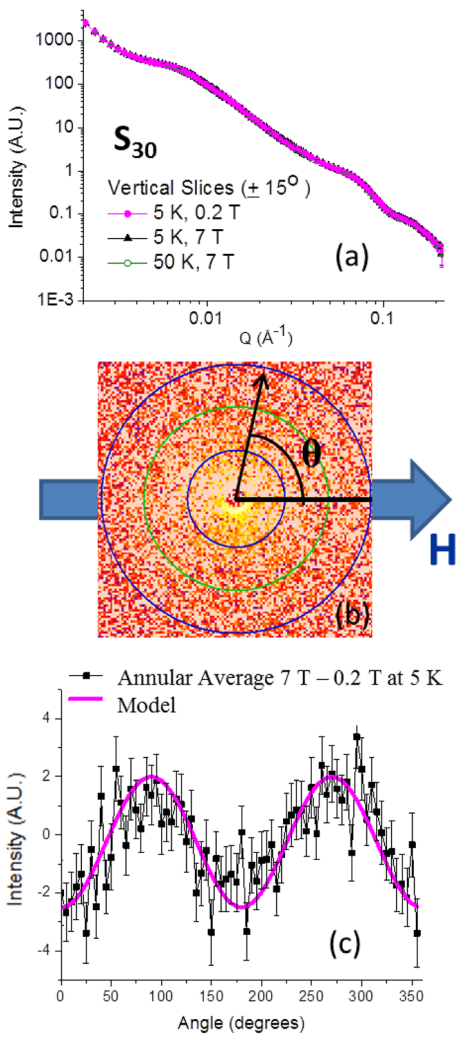

FIG. 2. (a) Vertical SANS ($\perp\vec{H}$) from S_{30}. (b) Two dimensional SANS image resulting from the difference of 7 T − 0.2 T at 5 K. (c) Annular average for 7 T–0.2 T at 5 K modeled with $2\sin^2(\theta)$ ($\propto M_{\parallel}$) − $2.5\cos^2(\theta)$ ($\propto M_{\perp}$), solid pink line.

difference was detected between −1.5 T and 1.5 T at 5 K, indicating that the effect of field direction is negligible. Yet, two-dimensional SANS patterns exhibit marked differences between 7 T and 0.2 T at 5 K, collected at three detector distances and summed together in Fig. 2(a). (Note there is a slight vertical shift between fields, but this has been effectively excluded in the annular average.) The annular variation (magnetic difference) between 7 T and 0.2 T at 5 K produces magnetic peaks at 90° and 270° and magnetic dips at 0° and 180° (Fig. 2(c)), which can be approximated with a $2\sin^2(\theta)\,(\propto M_{||})$ from the 7 T state minus $2.5\cos^2(\theta)\,(\propto M_{\perp})$ from the 0.2 T state.[21,22]

Scattering simplifies along the coordinate axes, where slices of ±15° are taken to improve counting statistics. Scattering about $0°, 180°$ contains $2 * |M_{\perp}|^2$, while scattering about $90°, 270°$ contains $|M_{||}|^2 + |M_{\perp}|^2$ components.[21,22] The $|M_{||}|^2$ scattering difference between 7 T and 0.2 T is shown in Fig. 3(a). It follows the general shape of the nanoparticle structural scattering. Conversely, the $|M_{\perp}|^2$ of 0.2 T–7 T increases between 5 K and 50 K, Fig. 3(b). Although the angular pattern of Fig. 2(c) is seen at all Q, the $|M_{\perp}|^2$ peaks at ≈0.006 Å^{-1} (inset of Fig. 3(b)) which would be consistent with magnetic scattering from a large feature, such as the γ-Mn_2O_3 shell, but not from the substantially smaller Fe_3O_4 cores or seeds. SQUID data (Fig. 3(c)) suggest that the T_C transition of γ-Mn_2O_3 occurs well below 50 K. Thus, the fact that large-scale (low-Q peaked) $|M_{\perp}|^2$ (Fig. 3(b)) develops above the apparent T_C of γ-Mn_2O_3 would be consistent with magnetic proximity effects[25] observed in MnO/γ-Mn_2O_3 and Fe_3O_4/γ-Mn_2O_3 core/shell nanoparticles, where γ-Mn_2O_3 was observed to remain magnetically ordered high above its T_C.[26,27]

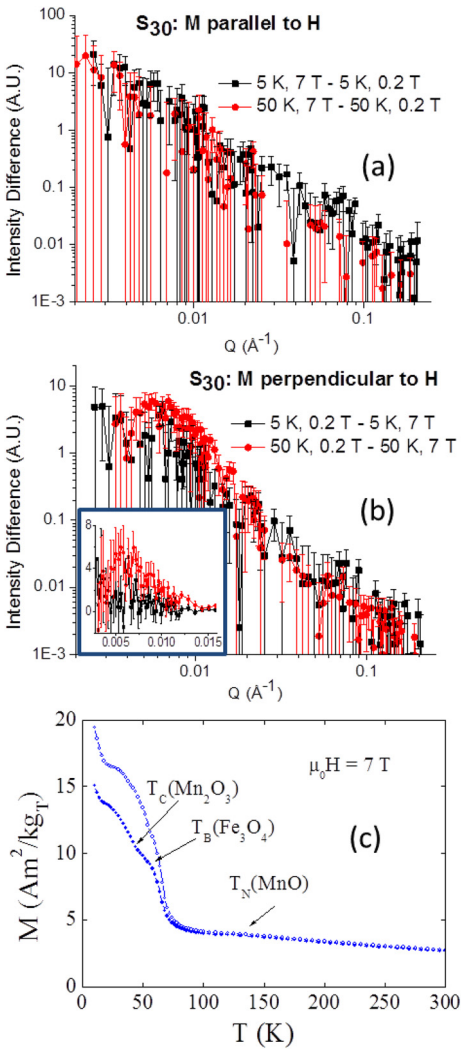

FIG. 3. S_{30} scattering for (a) $|M_{||}|^2$ and (b) $|M_{\perp}|^2$ (with linear-scale inset close-up). (c) SQUID magnetometry shown for field-cooling (top curve) and zero field cooling (bottom curve).

In summary, the magnetic reversals of FM/FM nanoparticles (S_0) and FM/AFM/FM nanoparticles (S_{30}), differing primarily in a 30 nm thick MnO AFM intermediate layer, are examined as a function of field and temperature. Increasing the temperature of S_0 to 100 K results in an enhancement of magnetism $\perp\vec{H}$ with a proportional reduction in magnetism $||\,\vec{H}$ (under a nominally saturating field of 1.25 T). A perpendicular magnetization component was observed at 5 K and 100 K, uniform within each particle at 100 K and longer-ranged at 5 K, suggesting that the graded FM layers rotate together. For S_{30}, exceeding the apparent T_C of γ-Mn_2O_3 (40 K) also gives rise to an enhancement of magnetism $\perp\vec{H}$ during magnetic reversal. The scattering associated with the perpendicular magnetization at 50 K, however, appears to originate primarily from the larger-scaled γ-Mn_2O_3 shell rather than the Fe_3O_4 cores or seeds based on its low-Q peak. This suggests a magnetization rotation within the shell that could be associated with a proximity effect in which T_C of the γ-Mn_2O_3 shell is enhanced above its bulk value.

This work has been supported by the 2009-SGR-1292 and MAT2010-20616-C02 of the Generalitat de Catalunya and the Spanish MINECO, respectively. M.E. thanks the Generalitat de Catalunya for her Beatriu de Pinós scholarship. M.D.B. acknowledges financial support from an ICREA-Academia Award. KLK and JAB thank Wangchun Chen and Shannon Watson for their assistance with the ^{3}He neutron spin filters.

[1]M. A. Willard *et al.*, Int. Mater. Rev. **49**, 125 (2004).
[2]X. Batlle and A. Labarta, J. Phys. D: Appl. Phys. **35**, R15 (2002).
[3]P. Tartaj *et al.*, J. Phys. D: Appl. Phys. **36**, R182 (2003).
[4]V. Skumryev *et al.*, Nature **423**, 850 (2003).
[5]J. Nogués *et al.*, Phys. Rep. **422**, 65 (2005).
[6]S. B. Darling and S. D. Bader, J. Mater. Chem. **15**, 4189 (2005).
[7]G. Salazar-Alverez *et al.*, J. Am. Chem. Soc. **129**, 9102 (2007).
[8]X. S. Liu *et al.*, Appl. Phys. A **77**, 673 (2003).
[9]O. Masala and R. Seshadri, J. Am. Chem. Soc. **127**, 9354 (2005).
[10]R. D. Rutledge *et al.*, J. Am. Chem. Soc. **128**, 14210 (2006).
[11]O. Masala *et al.*, Solid State Sci. **8**, 1015 (2006).
[12]A. López-Ortega *et al.*, Nanoscale **4**, 5138 (2012).
[13]G. S. Chaubey *et al.*, Chem. Mater. **20**, 475 (2008).
[14]G. Salazar-Alvarez *et al.*, J. Mater. Chem. **17**, 322 (2007).
[15]G. Salazar-Alvarez *et al.*, J. Am. Chem. Soc. **133**, 16738 (2011).
[16]L. Xi *et al.*, Nanotechnology **22**, 045707 (2011).
[17]J.-H. Lee *et al.*, Nat. Nanotechnol. **6**, 418 (2011).
[18]K. L. Krycka *et al.*, ACS Nano **7**, 921 (2013).
[19]S. Estradé *et al.*, Micron **43**, 30 (2012).
[20]C. L. Zha *et al.*, Appl. Phys. Lett. **97**, 182504 (2010).
[21]K. L. Krycka *et al.*, J. Appl. Crystallogr. **45**, 554 (2012).
[22]R. M. Moon, T. Riste, and W. C. Koehler, Phys. Rev. **181**, 920 (1969).
[23]S. R. Kline, J. Appl. Crystallogr. **39**, 895 (2006).
[24]A. J. Zambano *et al.*, Phys. Rev. B **75**, 144429 (2007).
[25]P. J. van der Zaag *et al.*, Phys. Rev. Lett. **84**, 6102 (2000).
[26]I. V. Golosovsky *et al.*, Phys. Rev. Lett. **102**, 247201 (2009).
[27]P. K. Manna *et al.*, J. Phys.: Condens. Matter **23**, 506004 (2011).